First-Generation Dendritic Polysilanes

Joseph B. Lambert,* Jodi L. Pflug, and John M. Denari

Department of Chemistry, Northwestern University, Evanston, Illinois 60208-3113

Received July 24, 1995[⊗]

Dendritic molecules have been constructed with only silicon−silicon linkages. Crystal structures have been obtained for three such molecules in which the core silicon is bonded to three silicons and each polysilyl wing branches once (one dendrimer generation). The three crystal structures differ in the number of spacer silicons between the core and the branch-point silicons and in the level of branching, which can be either 2-fold or 3-fold. Solution and mass spectral evidence was found for a fourth first-generation dendrimer. Despite having no all-anti pathway, these dendrimers show long-wavelength ultraviolet absorption. Because of the multiplicity of polysilane pathways, the ultraviolet absorption is intense, in one case 1 order of magnitude higher than for a comparable linear polysilane. The dendrimers are nonfluorescent at room temperature. The crystal structures provide quantitative data on numerous tetrasilane fragments, whose conformations fall into three families: gauche with dihedral angles in the range 30−64°, orthogonal with dihedral angles in the range 80−106°, and anti with dihedral angles in the range 131−177°.

A chain of silicon atoms bears little resemblance to an analogous chain of carbon atoms, as in polyethylene, beyond the formalities of tetravalency and saturation. The bonding between carbons within the polyethylene chain is very stable and resistant to a variety of reagents. There is little delocalization of electrons along the carbon chain, which lacks low-lying σ or π orbitals. In contrast, the Si−Si bonds in the silicon chain on the one hand are sensitive to a wide variety of conditions (electrophiles, nucleophiles, light,[1,2] heat[3]) but on the other hand offer some favorable electronic properties based largely on electron delocalization through the low-lying σ^* orbitals.[1,2] If greater robustness to the chemical environment can be achieved, polysilanes could be further exploited for their semiconductor,[4] photoconductor,[5] thermochromism,[6] and third-order nonlinear optical properties.[7] Exploration of these properties was made possible first by the preparation of well-characterized oligosilanes[8] and then by the construction of truly polymeric polysilanes.[9] By and large these materials were linear in structure, although some advances have been made in cross-linking.[10] Very few well-characterized branched polysilanes have been reported. For the one example with crystallographic data,[11,12] we will make structural comparisons herein.

In order to obtain a new, possibly more robust architecture for polysilanes, we have initiated a program for the preparation and characterization of dendritic polysilanes.[13] Dendrimer molecules emanate from a core with either three or four wings. Each wing branches again and again in a regular fashion, eventually to achieve a spherical shape.[14] The dendritic architecture has some advantages over linear polymers. First, in a spherical dendrimer, access of reagents to all the inner bonds is restricted or prohibited. One can then hope that dendritic polysilanes with methyl groups as the only substituents might present a largely methyl surface to reagents, with the more sensitive Si−Si bonds buried inaccessibly in the interior. The molecules would still be sensitive to light. Even if reagent exclusion is not perfect or if photochemical cleavage occurs, the large number of redundant pathways means that some molecular properties would survive the loss of portions of the molecule. We recently reported the first example of a dendritic polysilane.[13] Subsequently, the groups of Sakurai and Sekiguchi and of Suzuki prepared such materials.[15] Dendritic and hyperbranched siloxanes[16]

[⊗] Abstract published in *Advance ACS Abstracts,* December 15, 1995.

(1) West, R. In *The Chemistry of Organic Silicon Compounds*, Part 2; Patai, S., Rappoport, Z., Eds. Wiley: Chichester, U. K., 1989; pp 1207−1240.
(2) Michl, J.; Miller, R. D. *Chem. Rev.* **1989**, *89*, 1359−1410.
(3) Walsh, R. *Acc. Chem. Res.* **1981**, 246−252.
(4) West, R.; David, L. D.; Djurovich, P. I.; Stearley, K. L.; Srinivasan, K. S. V.; Yu, H. *J. Am. Chem. Soc.* **1981**, *103*, 7352−7354.
(5) Tachibana, H.; Matsumoto, M.; Tokura, Y.; Moritomo, Y.; Yamaguchi, A.; Koshihara, S.; Miller, R. D.; Abe, S. *Phys. Rev. B* **1993**, *47*, 4363−4371, and references cited therein.
(6) Yuan, C.-H.; West, R. *Macromolecules* **1994**, *27*, 629−630. Sakamoto, K.; Yoshida, M.; Sakurai, H. *Macromolecules* **1994**, *27*, 881−882.
(7) Kajzar, F.; Messier, J.; Rosilio, C. *J. Appl. Phys.* **1986**, *60*, 3040−3044.
(8) Kumada, M.; Tamao, K. *Adv. Organomet. Chem.* **1968**, *6*, 19−117. Allred, A. L.; Boberski, W. G. *J. Organomet. Chem.* **1975**, *88*, 65−72. Wesson, J. P.; Williams, T. C. *J. Poly. Sci., Poly. Chem. Ed.* **1979**, *17*, 2833−2843.
(9) West, R. *J. Organomet. Chem.* **1986**, *300*, 327−346. Kunai, A.; Kawakami, T.; Toyoda, E.; Ishikawa, M. *Organometallics* **1991**, *10*, 893−895, 2001−2003.
(10) Miller, R. D.; Hofer, D.; Sooriyakumaran, R.; Willson, C. G.; Fiskes, G. N.; Guillet, J. E.; Moore, J. *Polym. Mater. Sci. Eng.* **1986**, *55*, 599−603. Bianconi, P. A.; Weidman, T. W. *J. Am. Chem. Soc.* **1988**, *110*, 2342−2344.
(11) Lambert, J. B.; Pflug, J. L.; Allgeier, A. M.; Campbell, D. J.; Higgins, T. B.; Singewald, E. T.; Stern, C. L. *Acta Crystallogr. Sect. C* **1995**, *51*, 713−715.
(12) Ohshita, J.; Yoshitomi, T.; Ishikawa, M. *Organometallics* **1994**, *13*, 3227−3232. Whittaker, S. M.; Brun, M.-C.; Cervantes-Lee, F.; Pannell, K. H. *J. Organomet. Chem.* **1995**, *499*, 247−252.
(13) Lambert, J. B.; Pflug, J. L.; Stern, C. L. *Angew. Chem., Int. Ed. Engl.* **1995**, *34*, 98−99.
(14) Tomalia, D. A.; Naylor, A. M.; Goddard, W. A., III *Angew. Chem., Int. Ed. Engl.* **1990**, *29*, 138−175. Tomalia, D. A.; Durst, H. D. *Top. Curr. Chem.* **1993**, *165*, 193−313. Newcombe, G. R.; Yao, Z.-q.; Baker, G. R.; Gupta, V. K. *J. Org. Chem.* **1985**, *50*, 2003−2004. Newkome, G. R.; Moorefield, C. N.; Baker, G. R. *Aldrichimica Acta* **1992**, *25*, 31−38. Wooley, K. L.; Hawker, C. J.; Fréchet, J. M. *J. Am. Chem. Soc.* **1991**, *113*, 4252−4261.
(15) (a) Sekiguchi, A.; Nanjo, M.; Kabuto, C.; Sakurai, H. *J. Am. Chem. Soc.* **1995**, *117*, 4196−4197. (b) Suzuki, H.; Kimata, Y.; Satoh, S.; Kuriyama, A. *Chem. Lett.* **1995**, 293−294.

0276-7333/96/2315-0615$12.00/0

and carbosilanes[17] have been prepared by several groups, and Matyjaszewski et al.[18] have prepared highly branched polysilanes that may contain dendritic structures. We describe herein the preparation and characterization of several first-generation dendritic polysilanes.

Structural Variables and Nomenclature

For the special case of dendritic polysilanes, we have found a simple notation to be useful. Permethyl dendritic polysilanes build up rapidly and symmetrically from a single core atom. To this core, either three or four silicon atoms may be attached, and we refer to these possibilities as 3-fold core (C^3, a tridendron) and 4-fold core (C^4, a tetradendron), or C^c in general. The 2-fold example of course is excluded, as the result would be a linear polysilane rather than a dendrimer. The core silicon either is attached directly to the first branching silicon or is separated from it by any number of spacer dimethylsilyl groups. The spacer number S^s therefore may indicate zero spacer silicons (S^0), one spacer (S^1), and so on. At the first branch point there may be attached either two or three silicon atoms, referred to as 2-fold branching (B^2) or 3-fold branching (B^3), or B^b in general. Without these branch points, the result is not a dendrimer; the logical result of concatenation of single silicons is a star polymer (a core silicon atom with three or four straight chains emanating from it). A molecule with a symmetrically substituted core and a single branch point is a first-generation (G^1) dendrimer. After the branch there may be additional spacers followed by a second branch point, giving a second-generation (G^2) dendrimer. If there are *g* branch points (counting from the core), the generation is G^g. Core molecules such as $(Me_3Si)_4Si$ and $(Me_3Si)_3SiMe$ do not have dendritic structures, as they possess no branch point. Sometimes they are referred to as zeroth generation dendrimers because they can be elaborated into dendritic structures.

The complete structure of a first-generation polysilane dendrimer thus may be defined by three structural variables, the core multiplicity *c*, the spacer number *s*, and the branching number *b*. If the spacer and branching numbers are repeated identically in every generation, then only the generation number *g* need be added for a complete structural definition: $G^gC^cS^sB^b$ or ***gcsb*** in abbreviation. Figure 1 (methyl groups are implicit to complete valencies) illustrates the first-generation dendrimers with no spacer: the four possible results of 3-fold or 4-fold cores with 2-fold or 3-fold branching. We shall use ***gcsb*** ($g = 1, 2, 3, \ldots$; $c = 3$ or 4; $s = 0, 1, 2, \ldots$; $b = 2$ or 3) to represent these structures: **1302**, **1303**, **1402**, and **1403**. Figure 2 illustrates the four possible dendrimers with one silicon spacer: **1312**, **1313**, **1412**, and **1413**. These eight molecules comprise the subject of the present study. Additional families may be generated with any arbitrary number of spacers. Each of these molecules has higher generation analogues. Figure 3 illustrates the second-generation structure **2312**[15a] (3-fold core, one spacer, 2-fold branching). The structure is fully defined by the four numbers, so that the much more cumbersome name may be dispensed with: 6-[2′-

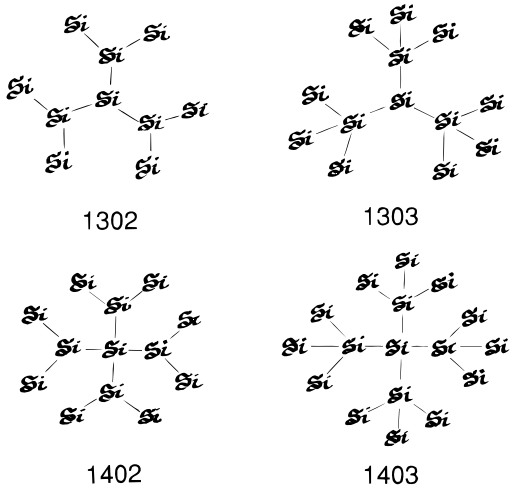

Figure 1. The family of first-generation permethyl dendritic polysilanes with no spacer between the core and the branch point.

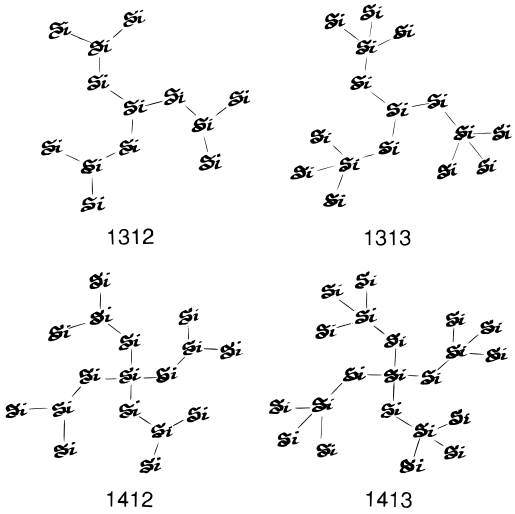

Figure 2. The family of first-generation permethyl dendritic polysilanes with one spacer silicon between the core and the branch point.

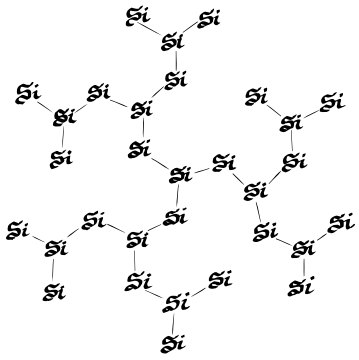

Figure 3. The second-generation permethyl dendritic polysilane with a 3-fold core, one spacer silicon, and 2-fold branching at each generational branch point, **2312**.

(16) Uchida, H.; Kabe, Y.; Yoshino, K.; Kawamata, A.; Tsumuraya, T.; Masamune, S. *J. Am. Chem. Soc.* **1990**, *112*, 7077−7079. Morikawa, A.; Kakimoto, M.-A.; Imai, Y. *Macromolecules* **1991**, *24*, 3469−3474. Mathias, L. J.; Carothers, T. W. *J. Am. Chem. Soc.* **1991**, *113*, 4043−4044. Seyferth, D.; Son, D. Y. *Organometallics* **1994**, *13*, 2682−2690.

(17) van der Made, A. W.; van Leeuwen, P. W. N. M. *J. Chem. Soc., Chem. Commun.* **1992**, 1400−1401. Zhou, L.-L.; Roovers, J. *Macromolecules* **1993**, *26*, 963−968. van der Made, A. W.; van Leeuwen, P. W. N. M.; de Wilde, J. C.; Brandes, R. A. C. *Adv. Mater.* **1993**, *5*, 466−468. Alonso, B.; Cuadrado, I.; Morán, M.; Losada, J. *J. Chem. Soc., Chem. Commun.* **1994**, 2575−2576. Caminade, A. M.; Majoral, J.-P. *Main Group Chem. News* **1995**, *3*, 14−24.

(18) Maxka, J.; Chrusciel, J.; Sasaki, M.; Matyjaszewski, K. *Macromol. Symp.* **1994**, *77*, 79−92.

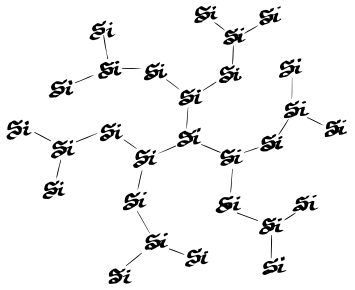

Figure 4. The second-generation permethyl dendritic polysilane with a 3-fold core and 2-fold branching, in which there is no spacer between the core and the first-generation branch point and one spacer silicon between the first and second-generation branch points, $G^2C^3S_1{}^0S_2{}^1B^2$.

[1″,1″,2″,3″,3″,3″-hexamethyl-2″-(trimethylsilyl)trisilyl]-1′,1′,2′,3′,3′,4′,5′,5′,5′-nonamethyl-4′-(trimethylsilyl)pentasilyl]-2,10-bis(trimethylsilyl)-4,8-bis[1′,1′,2′,3′,3′,3′-hexamethyl-2′-(trimethylsilyl)trisilyl]-1,1,1,2,3,3,-4,5,5,6,7,7,8,9,9,10,11,11,11-nonadecamethylundecasilane.

Certain structural features of these molecules are noteworthy and may be calculated directly from the four variables. The number P of terminal or peripheral silicon atoms is given by eq 1, the number L of silicon

$$P = cb^g \tag{1}$$

$$L = 3 + 2g + 2gs \tag{2}$$

$$T = 1 + c[b^g + (1 + s)\sum_{n=1}^{g} b^{(n-1)}] \tag{3}$$

$$M = 58T + 30 \tag{4}$$

atoms in the longest chain is given by eq 2, the total number T of silicon atoms is given by the series of eq 3, and the nominal molecular weight M is given by eq 4. These equations apply to any uniform dendrimer. For the molecule in Figure 3 of Sekiguchi et al.[15a] (**2312**), $L = 11$, $P = 12$, $T = 31$, and $M = 1828$. If the generations differ in spacer or branch number, these variables must be specified for each generation. Figure 4 illustrates a dendrimer that retains 2-fold branching but has no spacer in the first-generation and one spacer in the second ($G^2C^3S_1{}^0S_2{}^1B^2$). The expressions for the longest chain number and the total number of silicon atoms then are given by eqs 5 and 6, which apply to a system

$$L = 3 + 2g + 2\sum_{n=1}^{g} s_n \tag{5}$$

$$T = 1 + c[\sum_{n=1}^{g} (b^{(g-n)} + b^n s_{(n+1)})] \tag{6}$$

with variable spacer numbers but a constant branching number. If the branching number varies, the multiplicity of each branch point would have to be specified; e.g., $B_1{}^2$ and $B_2{}^3$ would signify 2-fold branching at the end of the first-generation portion and 3-fold branching at the end of the second-generation portion. We have not derived equations that include this structural complexity.

First-Generation Dendrimers with No Spacer

Figure 1 illustrates the four possible first-generation dendritic polysilanes lacking a spacer between the core and the branching point. These materials may be obtained by the reaction of either a 4-fold core precursor $SiCl_4$ or a 3-fold core precursor $MeSiCl_3$, both commercially available, with either a 3-fold branch extender $(Me_3Si)_3SiLi$ or a 2-fold branch extender $(Me_3Si)_2MeSiLi$ (Scheme 1) in a Wurtz-like coupling reaction. The

Scheme 1

$$MeSiCl_3 + 3(Me_3Si)_2MeSiLi \rightarrow \mathbf{1302}$$

$$MeSiCl_3 + 3(Me_3Si)_3SiLi \rightarrow \mathbf{1303}$$

$$SiCl_4 + 4(Me_3Si)_2MeSiLi \rightarrow \mathbf{1402}$$

$$SiCl_4 + 4(Me_3Si)_3SiLi \rightarrow \mathbf{1403}$$

lithium reagents tris(trimethylsilyl)silyllithium ("TrisLi")[19] and methylbis(trimethylsilyl)silyllithium ("BisLi")[20] are known, air-sensitive materials. Derouiche and Lickiss[21] carried out the reaction of TrisLi with $SiCl_4$ (a reaction that could give **1403**) and observed attachment of only one tris(trimethylsilyl)silyl group to the core silicon. This result suggests that steric requirements do not permit attachment of the remaining groups. A similar result seemed likely with the reaction of TrisLi with $MeSiCl_3$ (a reaction that could give **1303**), so we focused our attention on the reactions of BisLi to form dendrimers with 2-fold branching. The reaction of BisLi with $SiCl_4$, designed to produce **1402**, yielded as a primary product a substance with parent peak 522 rather than 784.

Finally, the reaction of BisLi with $MeSiCl_3$ successfully yielded the desired dendrimer **1302**, as well as a fragmentation product discussed later. Dendrimer **1302** is the least sterically demanding of the family illustrated in Figure 1, as it has a 3-fold core and 2-fold branching. The synthetic results indicate that in the absence of a spacer between the core and branch sites steric interactions are sufficient to hinder the formation of any but the least sterically demanding dendrimer.

Dendrimer **1302** has a total of 12 silicon atoms, a longest chain of 5 silicon atoms, 12 Si_5 pathways, 6 peripheral silicon atoms, and a nominal molecular weight of 726. Purification provided crystals suitable for X-ray analysis. The unit cell contained two independent molecules that differ insignificantly in structural parameters, which will be quoted herein as the mean of the two molecules. Figure 5 illustrates one of the molecules. The molecule has a propeller shape, with each blade pointing in the same sense (note the directions of methyl groups C2, C9, and C16 in Figure 5). Structural parameters indicate only light strain in the molecule. Most of the Si−Si bonds are within 0.1 Å of the normal value of 2.35 Å. Only the three bonds emanating from the core are slightly elongated: Si1−

(19) Gutekunst, G.; Brook, A. G. *J. Organomet. Chem.* **1982**, *225*, 1−3. Beno, M. A.; Hope, H.; Olmstead, M. M.; Power, P. P. *Organometallics* **1985**, *4*, 2117−2121.

(20) Baines, K. M.; Brook, A. G.; Ford, R. R.; Lickiss, P. D.; Saxena, A. K.; Chatterton, W. J.; Sawyer, J. F.; Behnam, B. A. *Organometallics* **1989**, *8*, 693−709.

(21) Derouiche, Y.; Lickiss, P. D. *J. Organomet. Chem.* **1991**, *407*, 41−49.

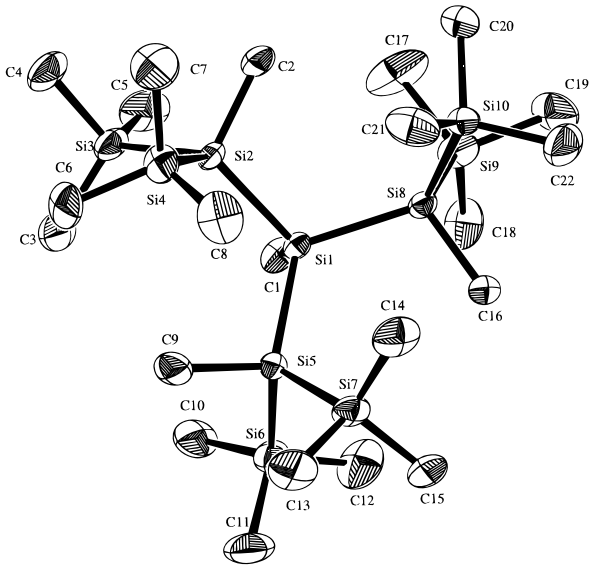

Figure 5. Molecular structure and numbering scheme for **1302**.

Table 1. Tetrasilane Dihedral Angles (deg) for 1302

OA	OO	AO	AG	GA	GO	OO	OG	OA	OO	GA	GO
93	93	133	133	33	33	100	100	95	95	30	30
132	102	95	30	132	103	95	30	131	103	131	103

Si2 2.367 Å, Si1−Si5 2.374 Å, and Si1−Si8 2.375 Å. Interaction between the three wings around the core is reduced by flattening the core (Si1) tetrahedron toward the methyl group (C1). The Si(branch)−Si1−Si(branch) angles average to 114.1°, and the Si(branch)−Si1−C1 angles average to 104.3°. Further relief of strain is achieved by opening up the Si1−Si(branch)−Si(TMS) angles to an average of 115.5° (one such angle, Si1−Si8−Si10 reaches 121.1°). These are not excessive values for the easily deformable Si−Si−Si angle, which is known to exceed 130°.[13]

The pentasilane pathways are defined by two dihedral angles. Teremae and Michl pointed out that tetrasilanes appear to exist in three conformational minima, in contrast to the common expectation of two for hydrocarbon chains (gauche and anti).[22] In silane chains, interactions between substituents, the higher deformability of Si−Si−Si angles, and possibly other factors serve to alter the dihedral angle of both the anti (from 180° to a lower value) and the gauche (from 60° to a smaller and a larger value). The changes thus create three conformational groupings, which Michl termed gauche (less than 60°), ortho or orthogonal (greater than 60°, or ∼90°), and anti (less than 180°). Table 1 lists the dihedral angles for the 12 pentasilane pathways in **1302**, each defined by two tetrasilane dihedral angles. There are a total of 12 roughly orthogonal (93−103°), 6 gauche (30−33°), and 6 anti (131−133°) arrangements, or as pentasilane pathways three each AO, GO, AG, and OO pathways.

First-Generation Dendrimers with One Spacer

Figure 2 illustrates the four possible dendrimers that have a single dimethylsilyl spacer group between the core silicon and the branching silicon. These molecules may be constructed by the reaction of the reagents BisLi or TrisLi with suitable chlorinated cores as depicted in Scheme 2. The two chlorinated cores were produced by the exchange of methyl for chlorine through treatment of tetrakis(trimethylsilyl)silane or methyltris(trimethylsilyl)silane with chlorotrimethylsilane in the presence of aluminum chloride.[23] This reaction selectively replaces a single methyl group (releasing tetramethylsilane) from each trimethylsilyl group with a chlorine atom to form chlorodimethylsilyl groups. Introduction of one chlorine deactivates the resulting chlorodimethylsilyl group from further chlorination. The reaction is easily followed by the evolution of the simple ^{1}H NMR spectrum of the symmetrical, fully chlorinated product. It was carried out successfully by way of practice on hexamethyldisilane (eq 7), and then on methyltris-(trimethylsilyl)silane (eq 8) and tetrakis(trimethylsilyl)-silane (eq 9). 1,2-Dichlorotetramethyldisilane (eq 7) was allowed to react with TrisLi to produce $(Me_3Si)_3SiSiMe_2$-$SiMe_2Si(SiMe_3)_3$ in 86% yield. We have already reported the structure of this highly branched, nondendrimeric molecule,[11] but we did not examine its structure previously for orthogonal conformations. The longest polysilane chain contains six silicon atoms, so each conformation is defined by three dihedral angles. The symmetry of the molecule requires a 180° dihedral angle for the central tetrasilane fragment, which is common to all the conformations. Table 2 gives the dihedral angles of the nine hexasilane pathways, rounded off. They clearly fall into three categories: gauche pathways with dihedral angles of 40°, orthogonal pathways with

Table 2. Tetrasilane Dihedral Angles (deg) for 2,2,5,5-Tetrakis(trimethylsilyl)-1,1,1,3,3,4,4,6,6,6-decamethylhexasilane

AAA	GAG	GAA	GAO	AAG	AAO	OAG	OAA	OAO
160	40	40	40	160	160	85	85	85
180	180	180	180	180	180	180	180	180
160	40	160	85	40	85	40	160	85

Scheme 2

$$MeSi(SiMe_2Cl)_3 + 3(Me_3Si)_2MeSiLi \rightarrow \mathbf{1312}$$

$$MeSi(SiMe_2Cl)_3 + 3(Me_3Si)_3SiLi \rightarrow \mathbf{1313}$$

$$Si(SiMe_2Cl)_4 + 4(Me_3Si)_2MeSiLi \rightarrow \mathbf{1412}$$

$$Si(SiMe_2Cl)_4 + 4(Me_3Si)_3SiLi \rightarrow \mathbf{1413}$$

$$Me_3SiSiMe_3 + Me_3SiCl \xrightarrow{AlCl_3} ClMe_2SiSiMe_2Cl + Me_4Si \quad (7)$$

$$(Me_3Si)_3SiMe + Me_3SiCl \xrightarrow{AlCl_3} (ClMe_2Si)_3SiMe + Me_4Si \quad (8)$$

$$(Me_3Si)_4Si + Me_3SiCl \xrightarrow{AlCl_3} (ClMe_2Si)_4Si + Me_4Si \quad (9)$$

(22) Teremae, H.; Michl, J. *Mol. Cryst. Liq. Cryst.* **1994**, *256*, 149−159.

(23) Ishikawa, M.; Kumada, M.; Sakurai, H. *J. Organomet. Chem.* **1970**, *23*, 63−69.

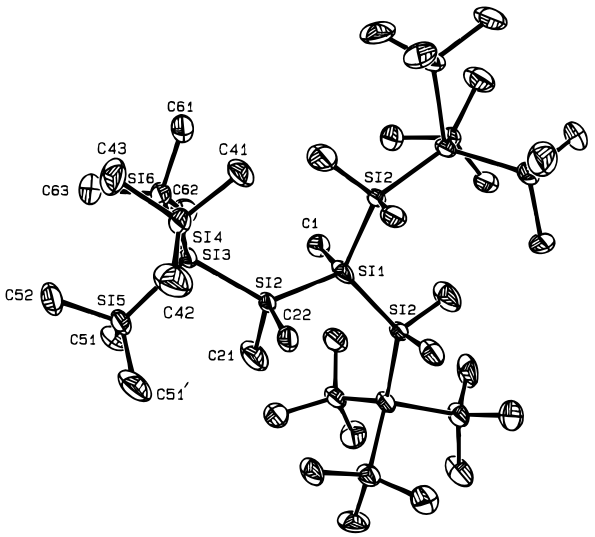

Figure 6. Molecular structure and numbering scheme for **1313**.

dihedral angles of 85°, and anti pathways with dihedral angles of 160 or 180°. There is one all-anti pathway (AAA), two each with two anti followed by either gauche (AAG) or orthogonal (AAO), two with OAG, and one each with GAG and OAO. As a result, the initial and final tetrasilane pieces are equally divided among the three forms (six each), and the central conformation is always anti.

The reaction of Scheme 2 to produce the least sterically hindered dendrimer, **1312**, with a 3-fold core and 2-fold branching was successful, although the material did not crystallize. This dendrimer has 13 silicon atoms, a longest chain of 7 silicons, 12 Si_7 pathways, and a nominal molecular weight of 868. The ^{29}Si spectrum supported the structure, and the highest molecular ion was at 855 $(M - 15)^+$ (the nominal $(M - 15)^+$ peak is at 853, but the buildup of C-13 and Si-29 makes the 854 and 855 peaks larger).

The reaction to produce **1412** yielded the dendrimer only as a very minor product, as demonstrated by a small molecular ion at 1018 (the nominal molecular ion has a mass of 1016). The structure of the major product was dendrimeric but arose from a fragmentation discussed in the next section.

The reaction of Scheme 2 for dendrimer **1313** proceeded in good yield to produce crystals that were able to be analyzed by X-ray crystallography (Figure 6). This molecule contains a total of 16 silicon atoms, a longest chain of 7 silicons that occurs 27 times, and a nominal molecular weight of 958. Two enantiomeric forms are present in the crystal. As with **1302**, the three wings are arranged like the blades of a propeller. There is considerable steric interaction between the individual neopentasilyl wings. To relieve this strain, the Si(core)−Si(spacer)−Si(branch) angle opens up considerably, to an average of 130.4°, and the Si(spacer)−Si(core)−Si(spacer) opens up to 116.1°. The latter angle implies that the tetrahedron around the core silicon is appreciably flattened toward the methyl group. If it had flattened fully so that the core and spacer silicons were in a single plane, the resulting trigonal geometry would have 360° for the sum of the Si(spacer)−Si(core)−Si(spacer) angles, compared with the observed value of 348.3° and the fully tetrahedral value of 328.5°. To accommodate this flattening, the Si(spacer)−Si(core)−CH_3 angle decreases to 101.54° and the angle between the geminal methyls on the spacer silicon decreases to 97.8°. One of the Si(spacer)−Si(branch)−$SiMe_3$ angles also opens up to 119.9°, but all other angles involving silicon or carbon are within 5° of tetrahedrality.

Table 3. Tetrasilane Dihedral Angles (deg) for 1313

OAGG	OAGA	OAGO	AAGO	AAGA	AAGG	GAGO	GAGA	GAGG
88	88	88	157	157	157	42	42	42
173	173	173	173	173	173	173	173	173
64	64	64	64	64	64	64	64	64
42	157	88	88	157	42	88	157	42

There is little strain left unrelieved by angle deformations. All Si−Si bond lengths are within 0.04 Å of the normal value of 2.34−2.35 Å. The longest Si−Si bond in the molecule is Si(spacer)−Si(branch) at 2.390 Å.

There are 27 heptasilane pathways, nine different ones in each of the three identical wings. A heptasilane fragment is defined by four dihedral angles that are given in Table 3 for **1313**. The nine sets of four are all different (OAGG, OAGA, OAGO, AAGO, AAGA, AAGG, GAGO, GAGA, GAGG) and are comprised of 15 anti arrangements (157−173°), 15 gauche arrangements (42−64°), and 6 orthogonal arrangements (88°).

The absorption maximum in the ultraviolet occurs at 272 nm, a value that is slightly longer than that of linear heptasilanes.[24] Moreover, the extinction coefficient at 3.4×10^5 is 1 order of magnitude larger than that in linear polysilanes with six to eight silicons. The energy and intensity of the absorption is remarkable since there is no all-anti pathway, which has been associated with optimal electronic delocalization in polysilanes.[25]

Fragmentations

In the course of the attempts to prepare the dendrimers illustrated in Schemes 1 and 2, we observed two products that appear to have come from sterically driven fragmentation reactions. In the first case, during the attempted preparation of **1412** (third reaction in Scheme 2), we isolated crystals whose structure by X-ray analysis proved to be $((Me_3Si)_2MeSiSiMe_2)_3SiH$. This structure is a dendrimer that differs from **1312**, which had been isolated but not crystallized, only in that the core silicon is attached to hydrogen rather than methyl. It is possible that the silyl hydride was produced by protonation of the anion $((Me_3Si)_2MeSiSiMe_2)_3Si:^-$ during hydrolytic workup. This anion in turn could have been formed from the reaction of the reagent anion BisLi on the chloride $((Me_3Si)_2MeSiSiMe_2)_3SiSiMe_2Cl$. This chloride is an expected intermediate from the third reaction in Scheme 2, at the point when the tetrachloride had reacted with only three molecules of BisLi. Attack of the fourth molecule of BisLi on the chlorinated silicon atom would have led to the desired **1412** with considerable increase in steric congestion. On the other hand, if BisLi displaced the hypothesized anion from the silicon instead of chloride, a reduction in steric congestion would occur, with formation of $(Me_3Si)_2MeSiSiMe_2Cl$ as a byproduct.

(24) Gilman, H.; Atwell, W. H.; Schwebke, G. L. *J. Organomet. Chem.* **1964**, *2*, 369−371.

(25) Plitt, H. S.; Downing, J. W.; Raymond, M. K.; Balaji, V.; Michl, J. *J. Chem. Soc., Faraday Trans.* **1994**, *90*, 1653−1662.

Table 4. Tetrasilane Dihedral Angles (deg) for 1312-H

AGAG	AOAA	OOAG	OOAA	AOAG	AOAA	GOAG	GOAA	AAOG	AAOA	OAOG	OAOA
132	132	106	106	177	177	61	61	132	132	106	106
80	80	80	80	84	84	84	84	154	154	154	154
151	151	151	151	147	147	147	147	89	89	89	89
61	177	61	177	49	169	49	169	49	169	49	169

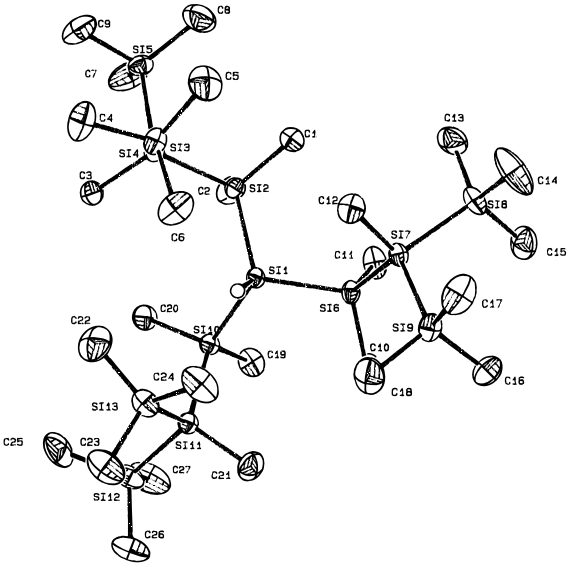

Figure 7. Molecular structure and numbering scheme for **1312**-H.

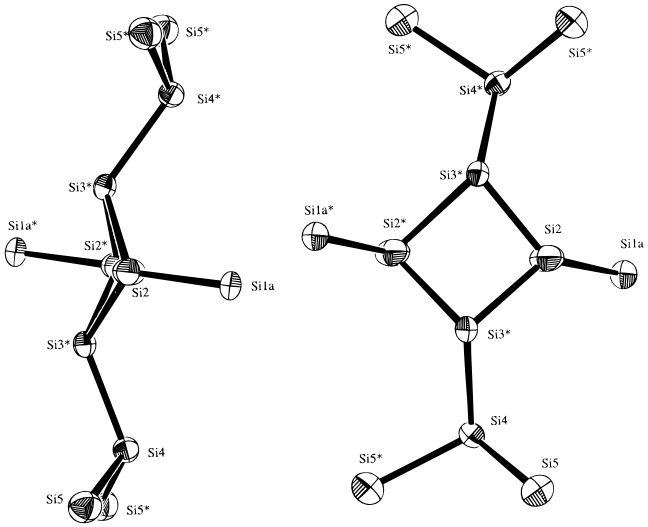

Figure 8. Molecular structure, showing substituent stereochemistry and ring conformation, and numbering scheme for *cis*,*cis*,*trans*-1,3-bis[1′-(trimethylsilyl)-1′,2′,2′,2′-tetramethyldisilyl]-2,4-bis(trimethylsilyl)-1,2,3,4-tetramethylcyclotetrasilane.

The structure of the hydridic product was supported by observation of the Si−H peak at δ 3.19 in the ^{1}H spectrum and of the expected parent peak at *m*/*z* 770 in the mass spectrum. X-ray crystallography confirmed the structure (Figure 7). We shall refer to the molecule as **1312**-H to indicate that hydrogen has replaced methyl on the core silicon. Nonetheless, it is a true first-generation dendritic polysilane with a total of 13 silicon atoms, 12 pathways along the longest chain of 7 silicons, and 6 peripheral silicons.

The hydridic hydrogen was refined isotropically to give a Si−H bond length of 1.45 Å. In contrast to **1302** and **1313**, each of the three wings is different. The Si−Si bond lengths were all within the range 2.34−2.37 Å. The average Si(spacer)−Si(core)−Si(spacer) angle of 111.4°, and their sum of 334.3° indicates little flattening about the central silicon tetrahedron. In contrast to the case for **1313**, the Si(core)−Si(spacer)−Si(branch) angle is not appreciably opened, the average being only 112.15°. Angles around the branching silicon also are not far from tetrahedral. These observations indicate that little strain needed to be relieved by bond and angle deformations.

Table 4 lists the Si−Si−Si−Si dihedral angles for **1312**-H, each heptasilane pathway being defined by four such numbers. Since the molecule does not have 3-fold symmetry, there is the maximum number of different pathways. There are three AOAA, two GOAA and AOAG, and one OOAA, OAOA, OOAG, OAOG, and GOAG pathways. The gauche angles fall in the range 49−61°, the orthogonal angles 80−106°, and the anti angles 132−177°. There is a greater preponderance of anti conformations in this molecule than in **1313**: 24 anti, 16 gauche, and 8 ortho arrangements.

The second example of apparent fragmentation occurred in the preparation of **1302**, which was accompanied by a substantial amount of a material whose X-ray crystal structure indicated that it was a cyclotetrasilane. Figure 8 provides two views of the molecule, showing both that it possesses a four-membered ring and that its four substituents alternate in the manner of a cis−cis−trans isomer (three up, one down). Methyl groups are omitted in the figure, so that the substituents may be seen clearly to have one and three silicon atoms, respectively, trimethylsilyl and heptamethylisopropasilyl groups. We found no trace of the other possible stereoisomers of the four-membered ring, in contrast to the case of a cyclotetragermane.[26]

Although we can make no definitive statement of the mechanism, it is interesting to hypothesize that the cyclotetrasilane formed by dimerization of a disilene, in this case $Me_3SiMeSi{=}SiMe((Me_3Si)_2MeSi)$. Disilenes[27] are known to undergo this reaction.[28] Whether our hypothetical disilene has the cis or trans stereochemistry is not known. Because of the fortunate presence of two different substituents on our disilene, we can state that its dimerization to the observed cyclotetrasilane would have to occur with $_\pi2_s + _\pi2_a$ stereochemistry to be allowed by orbital symmetry. This conclusion is true whether the disilene is cis or trans. It is unlikely that a nonconcerted reaction would give exclusively the sterically hindered cis−cis−trans isomer instead of the all trans or the cis−trans−cis. The disilene in turn could be produced during the first reaction of Scheme 1 ($MeSiCl_3$ with BisLi). Reaction with two molecules of BisLi produces the intermediate $((Me_3Si)_2MeSi)_2SiMeCl$. Reaction with the third molecule of BisLi would lead to

(26) Sekiguchi, A.; Yatabe, T.; Naito, H.; Kabuto, C.; Sakurai, H. *Chem. Lett.* **1992**, 1697−1700.

(27) Fink, M. J.; Michalczyk, M. J.; Haller, K. J.; West, R.; Michl, J. *Organometallics* **1984**, *3*, 793−800. Raabe, G.; Michl, J. *Chem. Rev.* **1985**, *85*, 419−509. West, R. *Pure Appl. Chem.* **1984**, *56*, 163−173.

(28) Gaspar, P. P.; Chen, Y.-S. *Organometallics* **1982**, *1*, 1410−1412.

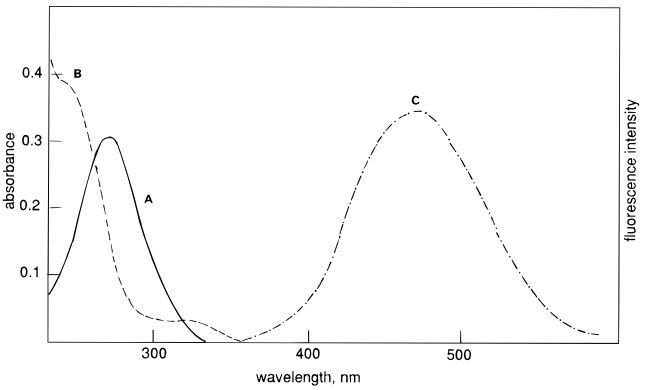

Figure 9. Ultraviolet absorption spectrum of **1313** in hexane at 298 K (A). Ultraviolet absorption spectrum in hexane at 298 K (B) and visible fluorescence spectrum in methylcyclohexane at 77 K (C) of the cyclotetrasilane.

Table 5. Electronic Properties of Polysilanes

polysilane	λ_{max}, nm	$10^{-5}\epsilon$	fl, nm[a]	Φ_f[a]
1302	240	0.25		
1313	272	3.4		
1312-H	259	0.64		$<10^{-3}$
CTS[b]	237 (320)[c]	0.43 (0.02)[c]	463	0.18
branch[d]	256	0.62	363	0.03
Si_6Me_{14}	260	0.25	363	0.45

[a] Fluorescence data 77 K, methylcyclohexane glass. [b] The cyclotetrasilane. [c] Shoulder. [d] 2,2,5,5-Tetrakis(trimethylsilyl)decamethylhexasilane.

Scheme 3

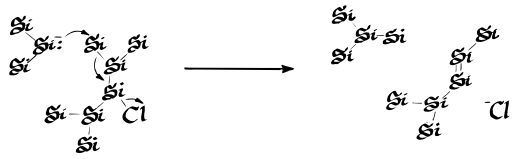

1302. A competing reaction involving attack of BisLi on a peripheral trimethylsilyl group would yield tris(trimethylsilyl)methylsilane, the hypothesized disilene, and chloride ion (Scheme 3). The resulting disilene would then dimerize to the observed product. Alternative mechanisms could occur, such as coupling of two molecules of $(Me_3Si)_2MeSi-SiMeCl-SiMe-SiMe_3$, but the observed stereochemistry of the product is a less likely result.

Absorption and Fluorescence Spectra

The dendrimers **1302**, **1313**, and **1312**-H, and the branched polysilane ($(Me_3Si)_3SiMe_2SiMe_2Si(SiMe_3)_3$) each display a single broad ultraviolet absorption band (see Figure 9 for **1313**). Maxima and extinction coefficients are reported in Table 5 along with data for the linear hexasilane and the cyclotetrasilane (**CTS**). Absorption maxima for linear polysilanes are known to increase with increasing chain length, reaching a limiting value of ~308 nm for permethylhexadecasilane.[31] In accord with this generalization we see an increase in λ_{max} for the series **1302** < branch < **1312**-H that parallels the increase in the longest polysilane chain from 5 to 6 to 7. A further increase in λ_{max} is observed for the dendrimer **1313**, even though the longest polysilane chain is the same as that in **1312**-H. Extinction coefficients also generally increase with increased branching, the value for **1313** being especially large. The large number of heptasilane pathways in **1313** may be responsible for the red-shifted, enhanced absorption.

The absorption spectrum of the cyclotetrasilane (Figure 9) displays a strong band at shorter wavelength than expected for a polysilane with a longest chain length of seven and a weaker long-wavelength shoulder. Similar absorption spectra have previously been reported by Shizuka et al.[32] for octakis(trialkylsilyl)-cyclotetrasilanes. The long-wavelength shoulder has been attributed to excitation from a delocalized σ orbital to a cyclobutane π orbital.[33]

The three polysilane dendrimers and the branched polysilane, like permethylhexasilane, are nonfluorescent at room temperature in dilute solution. Fluorescence quantum yields (Φ_f) and singlet lifetimes (τ_s) for permethylhexasilane decrease with decreasing temperature.[34] Values determined at 77 K in a methylcyclohexane glass are reported in Table 5. The increase in lifetime is attributed to a decrease in the rates of nonradiative processes, including Si−Si bond cleavage. Qualitatively similar behavior is observed for the branched polysilane. The values of Φ_f and τ_s at 77 K, however, are much smaller for this molecule than for permethylhexasilane (Table 5). The dendrimer **1313** is nonfluorescent at 77 K. The decrease in low-temperature lifetime for the series permethylhexasilane < branch < **1313** plausibly reflects an increase in photochemical reactivity with branching, as has previously been noted for branching of polysilanes.[35] Our preliminary studies of the photochemistry of the polysilane dendrimers indicate that they undergo rapid degradation to several volatile products on exposure to 254-nm light.

The cyclotetrasilane displays intense Stokes-shifted fluorescence at 77 K (Figure 9). Shizuka et al.[32] reported that the magnitude of the Stokes shift is dependent upon the planarity of the cyclotetrasilane ring. The fluorescence maximum of our cyclotetrasilane is more similar to that of the nonplanar tetraalkylcyclotetrasilanes than to the planar octakis(trialkylsilyl)-cyclotetrasilanes, in agreement with the X-ray structure.

Conclusions

First-generation dendritic polysilanes may be constructed by the synthetic procedures outlined in Schemes 1 and 2. These materials are stable in air at room temperature. Structures vary according to the core multiplicity, number of spacers, and branching multiplicity. Synthetic success is largely determined by the extent of steric strain in the transition states leading to formation of the dendrimer. We have been unable to isolate any dendrimer with 4-fold core multiplicity (C^4). In the absence of spacers (S^0), steric constraints

(29) Tomalia, D. A.; Naylor, A. M.; Goddard, W. A., III *Angew. Chem., Int. Ed. Engl.* **1990**, *29*, 138−175.
(30) de Gennes, P. G.; Hervet, H. J. *J. Phys. Lett.* (*Paris*) **1983**, *44*, 351−360.
(31) Sun, Y.-P.; Hamada, Y.; Huang, L.-M.; Maxka, J.; Hsiao, J.-S.; West, R.; Michl, J. *J. Am. Chem. Soc.* **1992**, *114*, 6301−6310.
(32) Shizuka, H.; Murata, K.; Arai, Y.; Tonokura, K.; Hiratsuka, H.; Matsumoto, H.; Nagai, Y. *J. Chem. Soc., Faraday Trans.* **1989**, *85*, 2809−2817.
(33) Grev, R. S.; Schaefer, H. F., III, *J. Am. Chem. Soc.* **1987**, *109*, 6569−6577.
(34) Sun, Y.-P.; Michl, J. *J. Am. Chem. Soc.* **1992**, *114*, 8186−8190.
(35) Harrah, L. A.; Zeigler, J. M. *Macromolecules* **1987**, *20*, 2037−2039.

Table 6. Structural Properties of Branched and Dendritic Polysilanes

	1302	**1312**	**1313**	**1312**-H	branch[a]
δ Si(core)	−44.4	−80	−69.6	−104	
δ Si(spacer)		−44.4	−26.7	−32.1	−29.8
δ Si(branch)	−76.3	−88.3	−124	−80.7	−128
δ Si(periphery)	−11.0	−12.8	−9.4	−11.3	−9.6
no. of Si atoms	12	13	16	13	10
longest Si chain	5	7	7	7	6
no. of longest chains	12	12	27	12	9
mol wt	612	868	961	772	612
Si−Si(core)−Si, deg	114.1		116.1	111.4	
Si−Si(spacer)−Si, deg			130.4	112.2	
Si−Si(core)−C, deg	104.3		101.5		
A:O:G[b]	6:12:6		15:6:15	24:8:16	6(15):6:6[c]

[a] 2,2,5,5-Tetrakis(trimethylsilyl)decamethylhexasilane. [b] Ratio of anti to orthogonal to gauche conformations. [c] The ratio is 15:6:6 for all arrangements but 6:6:6 if the nine anti arrangements around the central Si−Si bond are omitted.

are very high, so that only the doubly branched (B^2) dendrimer (**1302**) was able to be isolated. Steric effects on dendrimer formation previously were discussed in terms of de Gennes dense packing[29] and sterically induced stoichiometries.[30] In the presence of one spacer (S^1), both the doubly and triply branched dendrimers were isolated (**1312** and **1313**). Steric congestion was relieved by fragmentation reactions, in one case to form a smaller dendrimer than expected (**1312**-H, in which the core silicon bears a hydrogen rather than a methyl) and in another case possibly to form a disilene that dimerized to a cyclotetrasilane. Synthetic strategies for obtaining higher dendrimers should incorporate methods to reduce steric strain. The successful solution of the crystal structures of three dendrimers (**1302**, **1312**-H, and **1313**) indicated that strain was relieved primarily by angle distortion.

The ultraviolet maxima all occur at long wavelengths, despite the absence of any all-anti pathway (except in the branched molecule $(Me_3Si)_3SiSiMe_2SiMe_2Si(SiMe_3)_3$). Moreover, extinction coefficients range from slightly to significantly higher than in linear counterparts, presumably a result of the multiplicity of pathways. It is surprising that the absorption maxima and intensities are remarkably insensitive to the mix of anti, ortho, and gauche conformations.

Table 6 collects several properties of the four dendrimers that were isolated and characterized (one without an X-ray structure), as well as the branched polysilane (referred to in the table as "branch"). The ^{29}Si shifts in general are unremarkable, although the lower value for Si(spacer) in **1313** may be associated with the substantial increase in the Si(core)−Si(spacer)−Si(branch) angle with concomitant angle strain.

The crystal structures confirm the importance of orthogonal arrangements in polysilanes. The dihedral relationships in Tables 1−4 may be classified as gauche for the range 30−64°, ortho for the range 80−106°, and anti for the range 131−177°. No structures were observed with intermediate values, i.e., 65−79° and 107−130°. It is worth questioning whether a dihedral angle of 130° is properly termed anti. Although the range for antiperiplanar is generally defined as 180 ± 30°, that for anticlinal is 120 ± 30°. We have combined the upper end of anticlinal with the full range of antiperiplanar and simply termed them anti. The orthogonal range has been carved out of the interface between anticlinal (120 ± 30°) and gauche or synclinal (60 ± 30°).

Experimental Section

Tris(chlorodimethylsilyl)methylsilane.[23,36] A 250-mL, three-necked flask fitted with a Vigreux column distillation head was charged with methyltris(trimethylsilyl)silane[20] (2.0 g, 7.6 mmol), anhydrous $AlCl_3$ (∼0.5 g), and trimethylsilyl chloride (100 mL). The reaction was heated gently. After 10 min, tetramethylsilane began to distill. After slow reflux for 3 h, GC showed 95% conversion to the trichloride. The solution was allowed to cool. Dry acetone (2 mL) was added to precipitate the $AlCl_3$ that was then removed by filtration. Solvent was removed by distillation. The remaining brown oil was vacuum distilled to give 1.8 g (73%) of a colorless, opaque semisolid: ^{29}Si NMR (C_6D_6/C_6H_6) δ 26.0, −76.0; bp 94−96 °C (1.5 mm) (semisolid); MS (EI) *m/z* 324 (<1) (M^+), 309 (5), 287 (13), 267 (5), 231 (63), 229 (78), 194 (76), 151 (34), 131 (70), 116 (45), 93 (35), 73 (100).

Tetrakis(chlorodimethylsilyl)silane.[23,36] The procedure was the same as above but with tetrakis(trimethylsilyl)silane[37] (5.0 g, 0.016 mol), 1 g of $AlCl_3$, and 300 mL of trimethylsilyl chloride. Residual solvent was removed from the product under vacuum, leaving a white solid (6.4 g, 93%) which was sublimed (160 °C (0.3 mmHg) prior to further use: ^{1}H NMR ($CDCl_3$) δ 0.73 (s); ^{13}C NMR ($CDCl_3$) δ 6.6; ^{29}Si NMR (C_6D_6/C_6H_6) δ 28, −114; MS (EI) *m/z* 402 (0.6) (M^+), 387 (7.5), 367 (9), 309 (38), 272 (100), 229 (11), 209 (50), 194 (11), 174 (57), 131 (23), 93 (16), 73 (55).

2,4-Bis(trimethylsilyl)-3-[1′-(trimethylsilyl)-1′,2′,2′,2′-tetramethyldisilyl]nonamethylpentasilane (1302). In a 500-mL, three-necked flask, flushed with N_2, methyltris(trimethylsilyl)silane (25 g, 0.095 mol) in 250 mL of THF was converted to methylbis(trimethylsilyl)silyllithium.[20] The solution was cooled to 0 °C in an ice bath. A solution of methyltrichlorosilane (4.3 g, 0.288 mol) in THF (25 mL) was cooled to 0 °C and added to the lithium reagent over 15 min. The solution was allowed to stir overnight at room temperature. The solution was poured into 500 mL of dilute HCl. The organic layer was washed with 2 × 50 mL of H_2O. After drying over $MgSO_4$, the solution was concentrated to give a colorless, cloudy oil, which was vacuum distilled. The fraction distilling between 195 and 230 °C was collected (8 g). After sitting, the oil began to crystallize. The solid was isolated and recrystallized from benzene to yield two distinct crystal structures: long, columnar needles and boxy rhombohedra. The two solids proved to be *cis*,*cis*,*trans*-1,3-bis(1′-(trimethylsilyl)-1′,2′,2′,2′-tetramethyldisilyl)-2,4-bis(trimethylsilyl)-1,2,3,4-tetramethylcyclotetrasilane and $G^1C^3S^0B^2$, respectively. $G^1C^3S^0B^2$: ^{1}H NMR ($CDCl_3$) δ 0.31 (s, 18), 0.39 (s, 3), 0.64 (s, 1); ^{13}C NMR ($CDCl_3$) δ 1.86 (TMS), −6.26 (SiMe, branch), 0.38 (SiMe, core); ^{29}Si NMR ($CDCl_3$) δ −76, −44, −11; MS (EI) *m/z* 595 (<1) (M^+), 479 (2), 436 (26), 421 (33), 347 (6), 305 (19), 273 (26), 247 (98), 174 (100), 131 (25), 73 (78); λ_{max} = 240 nm; $\epsilon = 2.47 \times 10^4$ (hexane); 16% yield. Cyclotetrasilane: mp 151−6 °C, MS (EI) *m/z* 696 (M^+), 595, 507, 421 (100), 347, 273, 215; λ_{max} = 237 nm; $\epsilon = 4.3 \times 10^5$ (hexane); λ = 320 nm; $\epsilon = 2.3 \times 10^3$; 14% yield.

2,6-Bis(trimethylsilyl)-4-[2′-(trimethylsilyl)-1′,1′,2′,3′,3′,3′-hexamethyltrisilyl]undecamethylheptasilane (1312-H). A 250-mL, three-necked flask was flushed with N_2 and charged with methyltris(trimethylsilyl)silane (6.8 g, 0.026 mol) and THF (120 mL). Methylbis(trimethylsilyl)silyllithium was made according to a literature procedure.[19] The solution was cooled to 0 °C in an ice bath. Tetrakis(chlorodimethylsilyl)-silane (2.0 g, 4.9 mmol) was freshly sublimed, dissolved in THF

(36) Sakurai, H.; Watanabe, T.; Kumada, M. *J. Organomet. Chem.* **1967**, *9*, P11−P12.
(37) Gilman, H.; Smith, C. L. *J. Am. Chem. Soc.* **1964**, *86*, 1454.

(25 mL), and cooled to 0 °C. The chloride was added to the lithium reagent over 20 min. It was allowed to stir an additional 3 h on ice, overnight at room temperature, and then at 35−40 °C overnight. The solution was poured into 150 mL of dilute HCl. The organic layer was washed with saturated aqueous $NaHCO_3$. After drying over $MgSO_4$, the solution was concentrated and placed under 0.2 mmHg vacuum for 1 h. The remaining yellow oil (5.0 g crude, 132%) was dissolved in EtOH/acetone to yield 1.6 g (42%) of a white solid: mp 152−154 °C, ^{29}Si NMR (C_6D_6/C_6H_6) δ −11, −32, −80, −104; MS (EI) *m/z* 770 (M^+), 581, 522, 508, 449, 434 (100), 391, 376, 361, 318. Residual peaks for $G^1C^4S^1B^2$: MS (EI) *m/z* 1018 (M^+), 946, 857, 697, 508, 421 (100), 361. Anal. Calcd for $C_{27}H_{82}Si_{13}$: C, 42.00; H, 10.70. Found: C, 41.65; H, 10.78.

2,2,6,6-Tetrakis(trimethylsilyl)-4-[2′,2′-bis(trimethylsilyl)-1′,1′,3′,3′,3′-pentamethyltrisilyl]undecamethylheptasilane (1313). A 250-mL, three-necked flask was flushed with N_2 and charged with tris(trimethylsilyl)silyllithium (6 g, 13 mmol) and 20 mL of methyltetrahydrofuran freshly distilled from sodium. The solution was cooled to −15 °C in a salt/ice bath. Methyltris(chlorodimethylsilyl)silane (0.68 g, 2.1 mmol) was dissolved in 80 mL of methyltetrahydrofuran and cooled to −15 °C. The lithium reagent was added to the chloride over 20 min and was allowed to stir overnight as the bath warmed to 0 °C. The reaction was opened to the air while still cold and was allowed to warm to room temperature. The solution was poured into 100 mL of H_2O. The organic layer was washed with 100 mL of H_2O. After drying over $MgSO_4$, the solution was concentrated to a thick white oil that partially solidified upon sitting. The oil was dissolved in acetone to yield 1.7 g (85%) of a white solid: mp 150−60 °C, ^{13}C NMR (C_6D_6/C_6H_6) δ 4.0, −5.5; ^{29}Si NMR (C_6D_6/C_6H_6) δ −9, −27, −70, −124; MS (EI) *m/z* 945 ($M^+ - 15$), 711 (<1), 653 (<1), 638 (<1), 391 (52), 305 (100), 231 (37), 173 (24), 73 (46); $\lambda_{max} = 272$ nm; $\epsilon = 3.5 \times 10^5$.

2,6-Bis(trimethylsilyl)-4-[2′-(trimethylsilyl)-1′,1′,2′,3′,3′,3′-hexamethyltrisilyl]tridecamethylheptasilane (1312). A 500-mL, three-necked flask was charged with methyltris(trimethylsilyl)silane (16.2 g, 61.8 mmol) and 200 mL of THF. Methylbis(trimethylsilyl)silyllithium was made according to the literature.[19] The solution was cooled to 0 °C in an ice bath. Methyltris(chlorodimethylsilyl)silane (3.5 g, 11 mmol) was dissolved in 200 mL of THF and added dropwise to the lithium reagent over 35 min. The solution was stirred overnight at room temperature and then poured into 150 mL of dilute HCl. The organic layer was washed with H_2O, dried over $MgSO_4$, and concentrated to yield a yellow oil. The oil was dissolved in acetone and cooled in the refrigerator for several days. A thick colorless oil separated out and was isolated (∼6 g, 60%): ^{29}Si NMR ($CDCl_3$) δ −12.7, −88, −44, −80; MS (EI) *m/z* 785 (24) (M^+), 770 (32), 697 (39), 596 (58), 537 (60), 523 (100), 247 (64), 173 (78).

2,2,5,5-Tetrakis(trimethylsilyl)decamethylhexasilane. A 250-mL, three-necked flask was charged with tris(trimethylsilyl)silyllithium (2.4 g, 5.1 mmol) and 160 mL of pentane. 1,2-Dichlorotetramethyldisilane (0.35 g, 1.9 mmol) was dissolved in 40 mL of pentane and added to the lithium reagent. The solution began to cloud up immediately. It was allowed to stir overnight and then was poured into 300 mL of H_2O. The organic layer was dried ($MgSO_4$) and concentrated to yield 1.6 g (>100%) of crude solid. This material was recrystallized from EtOH/acetone to yield 1.0 g (86%) of a white solid: softens 250 °C, sublimes 255−260 °C; ^{1}H NMR (C_6D_6) δ 0.54 (s, 4), 0.33 (s, 18); ^{13}C NMR (C_6D_6) δ 3.7, 1.6; ^{29}Si NMR (C_6D_6) δ −9.6, −29.8, −128; MS (EI) *m/z* 610 (M^+) (6), 595 (6), 402 (11), 363 (34), 305 (100), 290 (49), 232 (26), 73 (19).

Crystal Structures. 1302. A colorless crystal of $Si_{10}C_{22}H_{66}$ was obtained from the slow evaporation at room temperature of a benzene solution. A platelike crystal was cut from the larger crystal. The resultant sample with approximate dimensions of 0.60 × 0.43 × 0.11 mm was mounted on a glass fiber using oil (Paratone-N, Exxon). All measurements were made on an Enraf-Nonius CAD4 diffractometer with graphite-monochromated Mo Kα radiation. Cell constants and an orientation matrix for data collection were obtained from a least-squares refinement using the setting angles of 25 carefully centered reflections in the range $20.0 < 2\theta < 23.8°$. The compound has a formula weight of 611.62, belonging to the primitive monoclinic space group $P2_1/c$ (No. 14) with a = 18.973(4) Å, b = 18.598(7) Å, c = 23.270(6) Å, Z = 8, V = 8204(3) Å^3, β = 92.27(2)°, and a calculated density of 0.99 g cm^{-3}. Diffraction intensities were collected using the $\omega-\theta$ scan technique to a maximum 2θ of 47.9°. Of the 13 670 reflections that were collected, 13 372 were unique (R_{int} = 0.056). The linear absorption coefficient for Mo Kα was 3.3 cm^{-1}. An empirical absorption correction (DIFABS) was applied that resulted in transmission factors of 0.93−1.06. Lorentz and polarization corrections were applied. A correction for a secondary extinction coefficient was applied (1.682×10^{-8}). The structure was solved by and expanded using Fourier techniques (DIRDIF92). Non-hydrogen atoms were refined anisotropically. Hydrogen atoms were included in fixed positions but not refined. The final cycle of full-matrix least-squares refinement was based on 5532 observed reflections ($I > 3.00\sigma(I)$) and 578 variable parameters and converged with unweighted and weighted agreement factors of R = 0.050 and R_w = 0.040. The maximum and minimum peaks on the final difference Fourier map corresponded to 0.38 and −0.32 e$^-$/Å^3, respectively. All calculations were performed using the teXsan crystallographic software package of Molecular Structure Corp.[38] Additional crystallographic details are included in the supporting information. Important structural parameters are given in Table 7.

1312-H. A colorless crystal of $Si_{13}C_{27}H_{82}$ was obtained from the slow evaporation at room temperature of a benzene solution. A crystal was cut from the larger crystal. The resultant sample with approximate dimensions of 0.65 × 0.63 × 0.34 mm was mounted on a glass fiber using oil (Paratone-N, Exxon). All measurements were made on an Enraf-Nonius CAD4 diffractometer with graphite-monochromated Mo Kα radiation. Cell constants and an orientation matrix for data collection were obtained from a least-squares refinement using the setting angles of 25 carefully centered reflections in the range $21.8 < 2\theta < 23.7°$. The compound has a formula weight of 772.06, belonging to the monoclinic space group $C2/c$ (No. 15) with a = 13.396(6) Å, b = 24.734(8) Å, c = 31.49(1) Å, Z = 8, V = 10381(11) Å^3, β = 95.70(3)°, and a calculated density of 0.988 g cm^{-3}. Diffraction intensities were collected using the $\omega-\theta$ scan technique to a maximum 2θ of 47.9°. Of the 8738 reflections that were collected, 8379 were unique (R_{int} = 0.127). The linear absorption coefficient for Mo Kα was 3.3 cm^{-1}. An analytical absorption correction was applied that resulted in transmission factors of 0.73−0.88. Lorentz and polarization corrections were applied. The structure was solved by direct methods (SHELXS-86). The hydrogen atom on Si(1) was refined isotropically. All other hydrogen atoms were included in fixed positions but not refined. Non-hydrogen atoms were refined anisotropically. The final cycle of full-matrix least-squares refinement was based on 6183 observed reflections ($I > 3.00\sigma(I)$) and 365 variable parameters and converged with unweighted and weighted agreement factors of R = 0.042 and R_w = 0.055. The maximum and minimum peaks on the final difference Fourier map corresponded to 0.62 and −0.43 e$^-$/A^3, respectively. All calculations were performed using the teXsan (version 5.0) crystallographic software package of Molecular Structure Corp.[38] Additional crystallographic details are included in the supporting information. Important structural parameters are given in Table 7.

1313. A colorless crystal of $Si_{16}C_{34}H_{102}$ with approximate dimensions of 0.4 × 0.2 × 0.2 mm was obtained from the slow evaporation at room temperature of a benzene solution and

(38) Molecular Structure Corp. 1989, teXsan. TEXRAY Structure Analysis Package. Version 5.0, 3200A Research Forest Drive, The Woodlands, TX 77381, 1989.

Table 7. Bond Lengths (Å) and Angles (deg) with Esd's

Bond Lengths for **1302**

Si(1)−Si(2)	2.363(3)	Si(6)−C(10)	1.873(7)	Si(1)−Si(5)	2.374(3)	Si(6)−C(11)	1.888(8)
Si(1)−Si(8)	2.377(3)	Si(6)−C(12)	1.872(9)	Si(1)−C(1)	1.903(6)	Si(7)−C(13)	1.866(8)
Si(2)−Si(3)	2.356(3)	Si(7)−C(14)	1.873(7)	Si(2)−Si(4)	2.358(3)	Si(7)−C(15)	1.875(8)
Si(2)−C(2)	1.904(7)	Si(8)−Si(9)	2.359(3)	Si(3)−C(3)	1.864(8)	Si(8)−Si(10)	2.365(3)
Si(3)−C(4)	1.874(8)	Si(8)−C(16)	1.898(7)	Si(3)−C(5)	1.882(8)	Si(9)−C(17)	1.868(8)
Si(4)−C(6)	1.869(8)	Si(9)−C(18)	1.875(8)	Si(4)−C(7)	1.860(8)	Si(10)−C(21)	1.861(8)
Si(4)−C(8)	1.873(8)	Si(10)−C(20)	1.862(7)	Si(5)−Si(6)	2.352(3)	Si(9)−C(19)	1.879(9)
Si(5)−Si(7)	2.360(3)	Si(10)−C(22)	1.870(8)	Si(5)−C(9)	1.909(7)		

Bond Angles for **1302**

Si(2)−Si(1)−S(5)	113.0(6)	Si(5)−Si(7)−C(13)	107.6(3)	C(6)−Si(4)−C(7)	108.3(4)	Si(8)−Si(9)−C(19)	108.1(3)
Si(2)−Si(1)−C(1)	105.0(2)	Si(5)−Si(7)−C(15)	112.1(2)	C(7)−Si(4)−C(8)	107.7(4)	Si(3)−Si(2)−Si(4)	107.8(1)
Si(2)−Si(3)−C(3)	113.9(2)	C(13)−Si(7)−C(15)	107.5(3)	Si(1)−Si(5)−Si(7)	118.4(1)	Si(4)−Si(2)−C(2)	105.6(2)
Si(3)−Si(2)−C(2)	102.9(2)	Si(1)−Si(8)−Si(9)	110.5(1)	Si(6)−Si(5)−Si(7)	107.0(1)	Si(2)−Si(3)−C(4)	107.5(2)
Si(5)−Si(1)−C(1)	104.2(2)	Si(1)−Si(8)−C(16)	108.0(2)	Si(7)−Si(5)−C(9)	107.8(2)	C(3)−Si(3)−C(4)	108.7(4)
Si(1)−Si(2)−Si(3)	110.68(1)	Si(9)−Si(8)−C(16)	102.3(2)	Si(5)−Si(6)−C(11)	107.5(3)	C(17)−Si(9)−C(19)	107.7(4)
C(3)−Si(3)−C(5)	108.9(4)	Si(2)−Si(1)−Si(8)	113.34(9)	C(10)−Si(6)−C(11)	106.3(3)	Si(8)−Si(10)−C(20)	113.7(2)
Si(2)−Si(4)−C(8)	114.2(2)	Si(5)−Si(1)−Si(8)	115.87(9)	C(11)−Si(6)−C(12)	109.3(4)	Si(8)−Si(10)−C(22)	105.6(3)
C(6)−Si(4)−C(8)	107.6(4)	Si(8)−Si(1)−C(1)	103.8(2)	Si(5)−Si(7)−C(14)	114.1(2)	C(20)−Si(10)−C(22)	107.4(3)
Si(1)−Si(5)−Si(6)	111.9(1)	Si(1)−Si(2)−Si(4)	120.3(1)	C(13)−Si(7)−C(14)	108.3(4)	C(20)−Si(10)−C(21)	106.0(3)
Si(1)−Si(5)−C(9)	108.3(2)	Si(2)−Si(3)−C(5)	111.0(3)	C(14)−Si(7)−C(15)	107.0(4)	C(21)−Si(10)−C(22)	108.3(4)
Si(6)−Si(5)−C(9)	102.2(2)	Si(1)−Si(2)−C(2)	108.1(2)	Si(1)−Si(8)−S(10)	121.4(1)	Si(8)−Si(9)−C(18)	109.9(3)
Si(5)−Si(6)−C(10)	111.8(2)	Si(2)−Si(4)−C(6)	112.6(3)	Si(9)−Si(8)−Si(10)	105.4(1)	C(17)−Si(9)−C(18)	110.5(4)
Si(5)−Si(6)−C(12)	113.8(3)	C(4)−Si(4)−C(5)	106.6(4)	Si(10)−Si(8)−C(16)	107.6(2)	C(18)−Si(9)−C(19)	106.2(3)
C(10)−Si(6)−C(12)	107.8(4)	Si(2)−Si(4)−C(7)	106.2(3)	Si(8)−Si(9)−C(17)	114.1(3)	Si(8)−Si(10)−C(21)	115.4(3)

Bond Lengths for **1313**

Si(1)−Si(2)	2.311(2)	Si(3)−Si(6)	2.353(7)	Si(5)−C(52)	1.878(8)	Si(2)−C(21)	1.768(7)
Si(2)−Si(3)	2.390(3)	Si(2)−C(22)	1.86(1)	Si(6)−C(61)	1.85(4)	Si(1)−C(1)	2.13(2)
Si(2)−Si(4)	2.365(6)	Si(4)−C(42)	1.88(1)	Si(6)−C(62)	1.83(1)	Si(4)−C(41)	1.88(3)
Si(3)−Si(5)	2.369(2)	Si(4)−C(43)	1.88(1)	Si(6)−C(63)	1.86(1)	Si(5)−C(51)	1.858(7)

Bond Angles for **1313**

Si(2)−Si(1)−Si(2′)	116.10(4)	Si(4)−Si(3)−Si(6)	16.7(1)	Si(2)−Si(1)−C(1)	101.54(7)	Si(3)−Si(5)−C(51)	111.9(2)
Si(2)−Si(1)−Si(2′)	23.1(1)	Si(5)−Si(3)−Si(6)	103.1(1)	Si(1)−Si(2)−Si(3)	130.4(1)	Si(3)−Si(5)−C(51)	111.9(2)
Si(2′)−Si(1)−Si(2″)	121.33(2)	Si(3)−Si(4)−C(41)	114(1)	Si(1)−Si(2)−C(21)	105.0(2)	Si(3)−Si(5)−C(52)	111.9(2)
Si(2)−Si(3)−Si(4)	113.2(1)	Si(3)−Si(4)−C(42)	111.9(4)	Si(1)−Si(2)−C(22)	102.2(3)	C(51)−Si(5)−C(51)	108.2(4)
Si(2)−Si(3)−Si(4)	132.2(1)	Si(3)−Si(4)−C(43)	107.9(4)	Si(3)−Si(2)−C(21)	110.7(3)	C(51)−Si(5)−C(52)	106.2(2)
Si(2)−Si(3)−Si(5)	104.69(9)	C(41)−Si(4)−C(42)	108(2)	Si(3)−Si(2)−C(22)	105.8(3)	Si(3)−Si(6)−C(61)	113(2)
Si(2)−Si(3)−Si(6)	119.9(1)	C(41)−Si(4)−C(43)	106(1)	C(21)−Si(2)−C(22)	97.8(3)	Si(3)−Si(6)−C(62)	109.6(4)
Si(2)−Si(3)−Si(6)	98.9(1)	C(61)−Si(6)−C(62)	110(1)	Si(2)−Si(3)−Si(2)	22.3(1)	Si(3)−Si(6)−C(63)	111.4(5)
Si(4)−Si(3)−Si(5)	106.2(1)	C(62)−Si(6)−C(63)	107.9(6)	C(42)−Si(4)−C(43)	108.0(6)	C(61)−Si(6)−C(63)	104.9(9)
Si(4)−Si(3)−Si(6)	108.4(2)						

Bond Lengths for **1312**-H

Si(1)−Si(2)	2.363(2)	Si(4)−C(4)	1.875(5)	Si(9)−C(18)	1.866(5)	Si(13)−C(22)	1.860(5)
Si(1)−Si(6)	2.360(2)	Si(4)−C(5)	1.867(5)	Si(10)−Si(11)	2.354(1)	Si(13)−C(23)	1.872(5)
Si(1)−Si(10)	2.366(1)	Si(4)−C(6)	1.870(4)	Si(10)−C(19)	1.888(4)	Si(13)−C(24)	1.874(4)
Si(1)−H(82)	1.45(4)	Si(5)−C(7)	1.857(5)	Si(10)−C(20)	1.889(4)	Si(5)−C(9)	1.868(5)
Si(2)−Si(3)	2.358(2)	Si(5)−C(8)	1.857(5)	Si(11)−Si(12)	2.346(2)	Si(6)−C(10)	1.883(4)
Si(2)−C(1)	1.894(4)	Si(6)−Si(7)	2.370(2)	Si(11)−Si(13)	2.344(2)	Si(7)−Si(8)	2.346(2)
Si(2)−C(2)	1.891(4)	Si(6)−C(11)	1.882(4)	Si(11)−C(21)	1.886(4)	Si(7)−C(12)	1.897(4)
Si(3)−Si(4)	2.355(2)	Si(7)−Si(9)	2.349(2)	Si(12)−C(25)	1.879(5)	Si(8)−C(14)	1.871(5)
Si(3)−Si(5)	2.354(2)	Si(8)−C(13)	1.873(5)	Si(12)−C(26)	1.888(5)	Si(8)−C(15)	1.876(5)
Si(3)−C(3)	1.902(4)	Si(9)−C(17)	1.879(5)	Si(12)−C(27)	1.878(5)	Si(9)−C(16)	1.862(4)

Bond Angles for **1312**-H

Si(2)−Si(1)−Si(6)	110.14(5)	Si(1)−Si(6)−C(11)	108.5(1)	C(16)−Si(9)−C(18)	109.1(2)	Si(7)−Si(9)−C(18)	110.4(1)
Si(2)−Si(1)−Si(10)	113.24(5)	Si(7)−Si(6)−C(10)	107.6(1)	Si(1)−Si(10)−Si(11)	111.94(5)	C(16)−Si(9)−C(17)	108.3(2)
Si(2)−Si(1)−H(82)	106(1)	Si(7)−Si(6)−C(11)	112.5(1)	Si(1)−Si(10)−C(20)	111.6(1)	C(17)−Si(9)−C(18)	106.8(2)
Si(6)−Si(1)−Si(10)	110.92(5)	C(10)−Si(6)−C(11)	106.1(2)	Si(11)−Si(10)−C(20)	107.0(1)	Si(1))−Si(10)−C(19)	109.2(1)
Si(6)−Si(1)−H(82)	112(2)	Si(6)−Si(7)−Si(8)	112.32(5)	Si(10)−Si(11)−Si(12)	109.46(5)	Si(11)−Si(10)−C(19)	110.5(1)
Si(10)−Si(1)−H(82)	105(1)	Si(6)−Si(7)−Si(9)	110.81(5)	Si(10)−Si(11)−C(21)	112.5(1)	C(19)−Si(10)−C(20)	106.4(2)
Si(1)−Si(2)−Si(3)	114.21(5)	Si(6)−Si(7)−C(12)	112.2(1)	Si(12)−Si(11)−C(21)	107.9(2)	Si(10)−Si(11)−Si(13)	112.13(5)
Si(1)−Si(2)−C(1)	110.3(1)	Si(8)−Si(7)−Si(9)	108.88(5)	Si(11)−Si(12)−C(25)	110.0(2)	Si(12)−Si(11)−Si(13)	108.15(5)
Si(1)−Si(2)−C(2)	107.5(1)	Si(2)−Si(3)−C(3)	112.4(1)	Si(11)−Si(12)−C(27)	112.7(2)	Si(13)−Si(11)−C(21)	106.5(1)
Si(3)−Si(2)−C(1)	106.8(1)	Si(4)−Si(3)−Si(5)	109.34(5)	Si(8)−Si(7)−C(12)	107.9(1)	Si(11)−Si(12)−C(26)	108.0(2)
Si(3)−Si(2)−C(2)	111.4(1)	Si(4)−Si(3)−C(3)	108.1(1)	Si(9)−Si(7)−C(12)	104.4(1)	C(25)−Si(12)−C(26)	109.3(2)
C(1)−Si(2)−C(2)	106.4(2)	Si(5)−Si(3)−C(3)	105.0(1)	Si(7)−Si(8)−C(13)	111.7(1)	C(25)−Si(12)−C(27)	108.8(2)
Si(2)−Si(3)−Si(4)	113.46(5)	Si(3)−Si(4)−C(4)	108.8(2)	Si(7)−Si(8)−C(14)	109.5(2)	Si(11)−Si(13)−C(22)	110.8(2)
Si(2)−Si(3)−Si(5)	108.17(5)	Si(3)−Si(4)−C(5)	111.3(2)	Si(7)−Si(8)−C(15)	111.4(1)	Si(11)−Si(13)−C(24)	110.1(2)
Si(3)−Si(5)−C(9)	110.6(2)	Si(3)−Si(4)−C(6)	113.8(1)	C(13)−Si(8)−C(14)	107.2(2)	C(22)−Si(13)−C(24)	109.9(2)
C(7)−Si(5)−C(8)	106.9(3)	C(4)−Si(4)−C(5)	108.1(2)	C(13)−Si(8)−C(15)	108.2(2)	C(26)−Si(12)−C(27)	108.0(2)
C(7)−Si(5)−C(9)	108.0(2)	C(4)−Si(4)−C(6)	107.0(2)	C(14)−Si(8)−C(15)	108.7(2)	Si(11)−Si(13)−C(23)	110.5(2)
C(8)−Si(5)−C(9)	107.8(2)	C(5)−Si(4)−C(6)	107.6(2)	Si(7)−Si(9)−C(16)	113.2(1)	C(22)−Si(13)−C(23)	108.8(2)
Si(1)−Si(6)−Si(7)	111.30(5)	Si(3)−Si(5)−C(7)	109.7(2)	Si(7)−Si(9)−C(17)	108.7(2)	C(23)−Si(13)−C(24)	106.6(2)
Si(1)−Si(6)−C(10)	110.7(1)	Si(3)−Si(5)−C(8)	113.7(2)				

was mounted on a glass fiber using oil (Paratone-N, Exxon). All measurements were made on an Enraf-Nonius CAD4 diffractometer with graphite-monochromated Mo Kα radiation. Cell constants and an orientation matrix for data collection were obtained from a least-squares refinement using the setting angles of 25 carefully centered reflections in the range $21.7 < 2\theta < 24.1°$. The compound has a formula weight of 960.55, belonging to the hexagonal space group $P6_3/m$ (No. 176) with $a = 15.020(3)$ Å, $c = 16.016(4)$ Å, $Z = 2$, $V = 3129(2)$ Å^3, and a calculated density of 1.019 g cm^{-3}. Diffraction intensities were collected using the $\omega-\theta$ scan technique to a maximum 2θ of 46.0°. Of the 3314 reflections that were collected, 2627 were unique ($R_{int} = 0.052$). The linear absorption coefficient for Mo Kα was 3.4 cm^{-1}. An analytical absorption correction was applied that resulted in transmission factors of 0.91−0.92. Lorentz and polarization corrections were applied. The structure was solved by direct methods (SHELXS-86). Non-hydrogen atoms were refined anisotropically. Hydrogen atoms on the carbon atoms located on the mirror plane were put in difference map positions. The remaining hydrogens were included in fixed positions but were not refined. The final cycle of full-matrix least-squares refinement was based on 1330 observed reflections ($I > 3.00\sigma(I)$) and 578 variable parameters and converged with unweighted and weighted agreement factors of $R = 0.059$ and $R_w = 0.061$. The maximum and minimum peaks on the final difference Fourier map corresponded to 0.51 and −0.46 e$^-$/Å^3, respectively. All calculations were performed using the teXsan (Version 5.0) crystallographic software package of Molecular Structure Corp.[38] Additional crystallographic details are included in the supporting information. Important structural parameters are given in Table 7.

Photochemistry. UV/visible absorption spectra were measured with a Hewlett-Packard Model 8452a diode array spectrophotometer in 1-cm path length quartz cuvettes. Fluorescence emission and excitation spectra were recorded using a Spex FluoroMax spectrophotometer in 1-cm path length quartz cells. Fluorescence quantum yields were determined relative to phenanthrene ($\Phi_f = 0.13$ in hexane[39]) for solutions of matched absorbance (∼0.1 OD). Solutions were ∼10^{-4} M and purged with nitrogen >5 min in 1-cm path length quartz cuvettes. Fluorescent lifetimes were measured with a PTI LS-1 spectrophotometer using a gated hydrogen arc lamp and single-photon-counting techniques.

Acknowledgments. The authors are grateful to the National Science Foundation for support of this work (Grant CHE-9302747), to C. L. Stern for solution of the crystal structures, and to Prof. F. D. Lewis for assistance with the photochemical experiments.

Supporting Information Available: Details of the crystal structures of **1302**, **1312**-H, and **1313** (99 pages). Ordering information is given on any current masthead page.

OM9505672

(39) Berlman, I. B. *Fluorescence Spectra of Organic Molecules*; Academic Press: New York, 1971.